IEEE Access
Multidisciplinary | Rapid Review | Open Access Journal

Received June 4, 2019, accepted July 1, 2019, date of publication July 3, 2019, date of current version July 24, 2019.

Digital Object Identifier 10.1109/ACCESS.2019.2926801

A Novel Algorithm for Robust Calibration of Kinematic Manipulators and Its Experimental Validation

CHENTAO MAO[1], SHUAI LI[2], (Senior Member, IEEE), ZHANGWEI CHEN[1], HONGFEI ZU[3], ZHIRONG WANG[1], AND YUXIANG WANG[1]

[1]State Key Laboratory of Fluid Power and Mechatronic Systems, Zhejiang University, Hangzhou 310058, China
[2]College of Engineering, Swansea University, Swansea SA2 8PP, U.K.
[3]School of Mechanical Engineering and Automation, Zhejiang Sci-Tech University, Hangzhou 310018, China

Corresponding author: Zhangwei Chen (chenzw@zju.edu.cn)

This work was supported by the 2017 National Key Research and Development Program of China under Grant 2017YFB1301400.

ABSTRACT Kinematic calibration of manipulators is an efficient and fundamental way to ensure reliability and high performance of robots. Research on kinematic calibration has a long tradition, and a common strategy used for calibration is to guarantee the least errors in the sense of root-mean-square deviation. However, the absolute positioning accuracy is determined by the maximum error of manipulators, and it is a key indicator for evaluating performance. For example, using manipulators to print machine elements, obviously where the error is the most, may likely cause inaccurate fit. Hence, it is crucial to study a robust calibration strategy. Considering the calibration problem, both positioning and orientation accuracy are ensured by minimizing the maximum positioning errors of three spherical mounted retro-reflectors (SMRs) on the end effector of manipulators. Unfortunately, traditional optimization methods based on gradient cannot be directly employed to solve the minimax problem. Due to the recent progress on optimization, researchers found that the minimax can be transformed into sequence quadratic programming problems under inequality conditions, thus providing solutions for solving the robust calibration. This paper applied this method to convert the calibration problem into constrained quadratic subproblems, and the subproblems can be solved through the primal-dual subgradient method. Then, convexity and robustness analysis is given to prove that these subproblems can quickly converge to a local minimum. Finally, to verify the validity of the proposed algorithm, the experiments are conducted on an IRB 2600 manipulator, and the results show that, with the minimax search algorithm, both the positioning and orientation accuracy is enhanced by 67.34% and 73.14%, respectively, which is significantly higher than the performance of the single-SMR calibration algorithm widely used in the field of industry.

INDEX TERMS Robot manipulators, kinematic calibration, robustness, pose accuracy.

I. INTRODUCTION

As critical components of modern manufacturing, industrial manipulators have been comprehensively applied in many fine-processing fields, such as precision assembling and operations [1]–[3], robotic machining [4], and vision-guided grasping [5], [6], which requires ultra-high precision of manipulators. However, due to the mechanical and geometrical reasons such as zero offset of joint angles and manufacturing deviation of rod lengths, the pose errors are unevenly distributed in the working space. Fortunately, the pose accuracy can be improved by kinematic calibration of robotic structural parameters. The field of kinematic calibration is maturing, with a wealth of well-understood methods and algorithms. Generally, kinematic calibration can be divided into two categories: self-calibration using redundant information and calibration with external sensors.

By constraining partial degrees of freedom (DOFs) of manipulators, self-calibration can realize the identification of structural parameters only through internal encoders of manipulator joints [7]–[9]. However, the parameter errors associated with constrained DOFs cannot be identified.

The associate editor coordinating the review of this manuscript and approving it for publication was Yangming Li.

TABLE 1. Comparisons among different methods for kinematic calibration.

♯	Positioning calibration	Orientation calibration	Optimization method	Modelling method	Handle constraints	Handle orientation
This paper	Yes	Yes	SQP, Primal-dual	MDH	Yes	minimize the worst case
Methods [18], [19]	Yes	No	Gauss-Newton	MDH	No	No
Methods [28]	Yes	Yes	Gauss-Newton	MDH	No	minimize pose
Methods [21]	Yes	No	Gauss-Newton	POE	No	No
Methods [20], [22]	Yes	Yes	Gauss-Newton	POE	No	minimize pose

Worse still, a large number of manual operations during the measurement process lead to inefficiency and inferior precision. Compared with the aforementioned self-calibration method, calibration with external sensors achieves higher accuracy and global volumetric error convergence since it directly optimizes the pose error of the points measured in the working space. Up to now, with the development of measurement technology, poses of manipulators can be attained by a lot of equipments, like laser tracker systems [10], vision systems with charge-coupled device (CCD) cameras [11], [12], 3-D laser scanner systems [13], [14] and so on. In [10], the authors identified joint errors and compensated the parameters to improve positioning accuracy through a laser tracker. Reference [15] compared the effects of kinematic calibration on the improvement of positioning accuracy based on different robot models. Similar researches in allusion to positioning accuracy can be found in [16]–[19].

Due to the lack of convenient measurement methods, less attention has been paid to orientation accuracy of manipulators than positioning accuracy in previous studies. Nevertheless, with a large orientation error, the positioning accuracy of manipulators will be significantly reduced when the end-effector is away from the calibrated point. Therefore, adding orientation information to the calibration process is of importance for improving performance of manipulators. In [20], a differential kinematics model of both position and orientation for calibration was proposed and established. Later in [21], the authors measured three points at the end-effector through a measurement arm, and calculated orientation errors for calibration. The positioning accuracy was found out to be worse than calibration with only position. Reference [22] similarly estimated orientation errors through pictures captured by two cameras, but there were still slightly large pose errors after calibration. In all of the three methods, a differential kinematics model of both position and orientation was established, and the calibration problem was described as a nonlinear least square problem solved by Gauss-Newton method. The objective function is the sum of weighted square of positioning and orientation errors of manipulators, and the selection of the weight coefficient will affect the results of the identification. In addition, the orientation is calculated by measured positions, which amplifies the measurement error.

In previous studies, we found that parameter errors can have a notable effect on the precise control of the robot [23]–[27]. In this paper, a novel kinematic calibration method based on optimization theory is proposed. A comparison of the proposed method with existing ones is shown in TABLE 1. Instead of calculating orientation errors directly, by minimizing the maximum positioning errors of three points, both positioning and orientation accuracy can be guaranteed in this method. With the constraint of distance invariance, the minimax problem can be redefined as a sequence quadratic programming (SQP) problem with fast local convergence through primal-dual subgradient method. In the meantime, robustness of the calibration process is increased by introducing the minimax search algorithm.

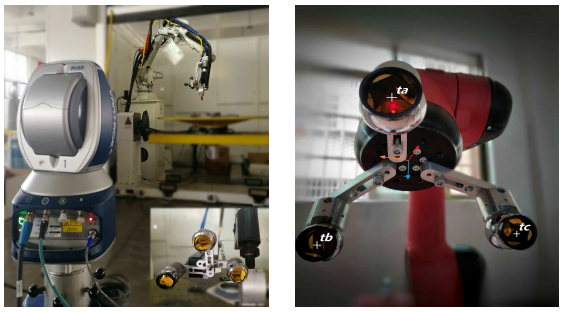

(a) (b)

FIGURE 1. Experimental apparatus for manipulator kinematic calibration in our lab. (a) Physical map of a laser tracker, FARO Vantage, and an ABB IRB 2600 manipulator. (b) The installation position of SMRs: *ta*, *tb* and *tc* are the three-dimensional Cartesian coordinates of the three SMRs expressed in the end-effector coordinate system.

The remainder of this paper is divided into four sections. In Section II, the minimax problem with constraints is formulated. In Section III, the problem in Section II is approximately redefined as a quadratic programming problem with fast local convergence, and convergence of the optimization problem is analyzed. Section IV illustrates the experimental results including comprehensive comparisons among different methods. Section V summarizes this paper.

II. ROBUST CALIBRATION PROBLEM FORMULATION

In this section, definitions on manipulator kinematics and description of pose accuracy are presented for problem formulation. The objective function for robust calibration and constraints based on distance invariance are proposed.

A. SENSOR-ROBOT SYSTEM

The experimental system setup is presented in Fig. 1, where the pose measurement is achieved by measuring the positions

of three SMRs mounted on the end flange of the manipulator. The manipulator attains m arbitrary configurations in succession. And then, the positions of the SMRs are measured by a laser tracker in each configuration, and in the meantime, the corresponding joint angles are recorded.

The position y of the end-effector is expected to reach the desired point y_d. Unfortunately, due to the mechanical and geometrical reasons such as the zero offset of joint angles and the manufacturing deviation of rod lengths, the end-effector errors are unevenly distributed in the working space resulting in positioning errors of the three SMRs. Consider the three SMRs as a unified whole for pose measurement as shown in Fig. 1(b). According to geometry theroy, it is known that the position and orientation of a plane can be fixed by constraining the positions of three points on a plane that are not collinear. So, minimizing the maximum value of the positioning errors of three SMRs can improve both positioning and orientation accuracy of the end-effector, furthermore the robustness of algorithm is improved by introducing the minimax search method. Clearly, the distance between any two of the three SMRs is fixed physically and can be measured by a laser tracker, which can be treat as a constraint for optimization problems.

The calibration process is an offline process, and the manipulators that need to be calibrated are those that have been assembled waiting to be shipped from the factory or have been used for a long time, with zero offsets or deformation of the rods. By the kinematic calibration process, the end-effector errors due to structural parameter errors can be minimized.

B. FORWARD KINEMATICS

Considering an n-DOF manipulator, the Cartesian coordinate of the end point can be analytically described as a nonlinear mapping

$$y = f(\theta, x), \tag{1}$$

where the mapping $y(\cdot)$ provides the connection between the joint angle $\theta = [\theta_1, \theta_2, \ldots \theta_n]^{\mathrm{T}}$, the structural parameters $x \in R^{g\times 1}$ on the joint space and the position of end point on the Cartesian space. Take the differential on both sides of (1), we can yield

$$dy = \frac{\partial f(\theta, x)}{\partial x^{\mathrm{T}}} dx = J(\theta, x)dx, \tag{2}$$

where $J(\theta, x) \in R^{3\times g}$ is called the Jacobian matrix of the manipulator, and usually is abbreviated as J.

C. POSITIONING AND ORIENTATION ACCURACY

The positioning accuracy of a robot manipulator is defined below, namely the end-effector errors

$$AP = \|ym - y\| = \|ym - f(\theta, x)\|, \tag{3}$$

where y is the coordinate of the command position, which can be calculated by substituting structural parameters x and joint angle values θ of the manipulator into the formula (1); ym is the coordinate of the attained position.

The orientation accuracy defined in ISO9283 is described as formula (4) by the deviation of Euler angles.

$$AO = [|a_m - a_c|, |b_m - b_c|, |c_m - c_c|], \tag{4}$$

where the orientation of the manipulators is referred as a, b, c values, the angular components about axes $x - y - z$, and the subscript m and c indicate the measured and calculated value of the orientation, respectively. Using scalar deviation to denote orientation accuracy, there is no comparability between different configurations of manipulator, worse still, the orientation accuracy does not reflect the real situation when the Euler angles are near the singular configuration. To overcome the above disadvantages, a new orientation accuracy indicator [22] of a robot manipulator is given by

$$AO' = \|log(R_m^{\mathrm{T}} R_c)^{\vee}\|, \tag{5}$$

where the orthogonal matrix R represents the orientation transformation from the base coordinate system of the manipulator to the end-effector coordinate system, and $log(R_m^{\mathrm{T}} R_c)^{\vee} \in R^3$ denotes the vector representation of $log(R_m^{\mathrm{T}} R_c) \in so(3)$.

D. OPTIMIZATION PROBLEM FORMULATION

The objective function of the optimization is defined as minimizing the maximal error of three points (SMRs), where the error is expressed by the sum of the squares of the positioning errors corresponding to the m configurations, which can be calculated by

$$F(x) = r^{\mathrm{T}} r = \sum_{j=1}^{m} [r_j(x)]^2 = \sum_{j=1}^{m} \|ym_j - f(\theta_j, x)\|^2, \tag{6}$$

where $r = [r_1, \ldots, r_m]^{\mathrm{T}}$ is the sequence of positioning accuracy. Both accuracy and robustness should be thought and made to the optimal trade-off in the choice of the indicator function containing the errors of three SMRs. Hence, a minimax search algorithm is chosen to solve the above problem

$$\begin{aligned} &\min_x \max_i : \ F_i(x), \\ &subject\ to : \ c(x) \le 0, \end{aligned} \tag{7}$$

where the subscript i indicates $i-th$ SMR, and $c(x) \le 0$ is the inequality constraint defined in Section II-E. By optimizing the structure parameters x, such as link lengths, joint offsets, and the transformation of coordinate systems, the goal can be achieved.

E. NONLINEAR INEQUALITY CONSTRAINT

Clearly the three SMRs are fixed on the flange, and the distances between any two of them are independent of the coordinate system. So, the distance of two SMRs in the end flange coordinate system is equal to the corresponding distance measured by the laser tracker. However, considering

measurement errors, the distance invariance can be expressed as an inequality constraint

$$\begin{cases} (rt_1)^2 = [\|ta - tb\| - \dfrac{1}{m}\sum_{j=1}^{m}\|ym_{1j} - ym_{2j}\|]^2 \le \epsilon, \\ (rt_2)^2 = [\|tb - tc\| - \dfrac{1}{m}\sum_{j=1}^{m}\|ym_{2j} - ym_{3j}\|]^2 \le \epsilon, \\ (rt_3)^2 = [\|tc - ta\| - \dfrac{1}{m}\sum_{j=1}^{m}\|ym_{3j} - ym_{1j}\|]^2 \le \epsilon, \end{cases} \tag{8}$$

where $rt_l, l = 1, 2, 3$ is the deviation of the nominal and the measured distance between any two SMRs in the $l - th$ group, and l is the number of nonlinear constraints. ta, tb and tc are the nominal three-dimensional Cartesian coordinates of the three SMRs expressed in the end coordinate system of the manipulator. The measured distances are acquired by averaging m measurements. The error value between the nominal and the measured of the distance is set to less than a threshold, ϵ. The formula (8) can be rewritten as

$$c(x) = \begin{bmatrix} (rt_1)^2 - \epsilon \\ (rt_2)^2 - \epsilon \\ (rt_3)^2 - \epsilon \end{bmatrix} \le 0, \tag{9}$$

Hence, taking into account the minimization of maximum positioning errors and distance invariance, the robust calibration problem can be transformed into a minimax problem with constraints.

III. MINIMAX SEARCH ALGORITHM WITH SQP APPROACH

In this section, we redefine the minimax problem with nonlinear inequality constraints as a SQP subproblem, and solve the SQP subproblem with primal-dual subgradient method.

A. REDEFINITION OF THE OBJECTIVE FUNCTION

The problem, $\min\limits_{x}\max\limits_{i} : F_i(x)$, can be equated to a minimization problem with constraints:

$$\begin{aligned} &\underset{x}{minimize} : \ \phi(x), \\ &subject\ to : \ F_i(x) \le \phi(x), \end{aligned} \tag{10}$$

where $\phi(x) = \max\limits_{i}\{F_i(x)\}$. One of approaches to solve the above constrained problem is to solve the approximate quadratic programming (QP) problem iteratively by generating a sequence $\{x^k\}$ which converges to the solution, namely SQP method [29]–[31]. The main idea here is to linearize the original system and to solve the resulting linear problem with fast local convergence. Owing to $F_i(x)$ differentiable, then, for any direction Δx, the directional derivative $D_{\Delta x}\phi(x)$ can be expressed as

$$D_{\Delta x}\phi(x) = \max_{i\in I(x)}\{\nabla F_i^{\mathrm{T}}(x)\Delta x\}, \tag{11}$$

where

$$I(x) = \{i : \ F_i(x) = \phi(x)\}, \tag{12}$$

The step Δx can be obtained by

$$\begin{aligned} &\underset{\Delta x}{minimize} : \ \frac{1}{2}\Delta x^{\mathrm{T}} H_k \Delta x + D_{\Delta x}\phi(x^k), \\ &subject\ to : \ F_i(x^k) + \nabla F_i^{\mathrm{T}}(x^k)\Delta x \le \phi(x^k) + D_{\Delta x}\phi(x^k), \end{aligned} \tag{13}$$

where the Hessian matrix H_k updated through BFGS method is positive definite, $\Delta x = x^{k+1} - x^k$. Taking a close observation of (13), we notice that when $\Delta x = 0$, then, $D_{\Delta x}\phi(x) = 0$, the new objective function gets the value of zero; when $\Delta x \ne 0$, since H_k is positive definite, then, $\Delta x^{\mathrm{T}} H_k \Delta x > 0$, and hence $D_{\Delta x}\phi(x) < 0$. Thus, the following relationship can be obtained by expanding at x^k and using the constraint condition in (13)

$$\begin{aligned} F_i(x^k + \delta\Delta x) &= F_i(x^k) + \delta\nabla F_i^{\mathrm{T}}(x^k)\Delta x + O(\delta^2) \\ &\le \phi(x^k) + \delta D_{\Delta x}\phi(x^k) + O(\delta^2) < \phi(x^k), \end{aligned} \tag{14}$$

Hence, Δx is a descent direction, and there exists some sufficiently small $\delta \ge 0$ such that

$$\max_i\{F_i(x^k + \delta\Delta x)\} < \max_i\{F_i(x^k)\}, \tag{15}$$

B. REDEFINITION OF THE INEQUALITY CONSTRAINT

The minimax problem with constraints can be stated in terms of the minimizing problem defined as

$$\begin{aligned} &\underset{x}{minimize} : \ \phi(x), \\ &subject\ to : \ F_i(x) - \phi(x) \le 0, \\ &\qquad\qquad c(x) \le 0, \end{aligned} \tag{16}$$

where the inequality constraints can be combined into

$$C_I(x) = \begin{bmatrix} F_i(x) - \phi(x) \\ c(x) \end{bmatrix}, \tag{17}$$

For a constrained optimization problem, the Karush-Kuhn-Tucker (KKT) equations are necessary conditions. Commonly, the SQP method can be applied to solve the constrained quasi-Newton problem, since the superlinear convergence is guaranteed by accumulating second-order information regarding the KKT equations. Combining formula (11), the osculating QP subproblem can be deduced as

$$\begin{aligned} &\underset{\Delta x}{minimize} : \ \frac{1}{2}\Delta x^{\mathrm{T}} H_k \Delta x + D_{\Delta x}\phi(x^k), \\ &subject\ to : \ \nabla F_i^{\mathrm{T}}(x^k)\Delta x - D_{\Delta x}\phi(x^k) \\ &\qquad\qquad +F_i(x^k) - \phi(x^k) \le 0, \\ &\qquad\qquad \nabla c^{\mathrm{T}}(x^k)\Delta x + c(x^k) \le 0, \end{aligned} \tag{18}$$

Here, the Lagrangian is defined as

$$\begin{aligned} L(\Delta x, \lambda) \triangleq \frac{1}{2}\Delta x^{\mathrm{T}} H_k \Delta x + D_{\Delta x}\phi(x) \\ +\lambda^{\mathrm{T}}(C_I(x) + G(x)\Delta x), \end{aligned} \tag{19}$$

where $\lambda \geq 0$ are called Lagrange multipliers, and G(x) is the gradient of the inequality constraints $C_I(x)$. For optimal Δx^* it must hold the KKT conditions (necessary condition) of (18)

$$\begin{cases} \nabla F_i(x)|_{i\in I(x)} + H_k \Delta x + \left(G^{\mathrm{T}}(x)\right)^+ \lambda = 0, \\ \left(C_I(x) + G(x)\Delta x\right)^+ = 0, \\ \lambda \geq 0, \\ (\lambda)^{\mathrm{T}}\left(C_I(x) + G(x)\Delta x\right) = 0, \end{cases} \tag{20}$$

where $(\cdot)^+$ is defined as

$$(x)^+ = \begin{cases} x, x \geq 0, \\ 0, x < 0, \end{cases} \tag{21}$$

The step size along the descent direction and the step length of Lagrange multipliers can be determined through primal-dual subgradient method, where $(\Delta x, \lambda)$ is primal-dual optimal if and only if

$$\begin{cases} 0 \in \partial_{\Delta x} L(\Delta x^p, \lambda^p) = H_k \Delta x^p + \nabla F_i(x^k)|_{i\in I(x)} \\ \qquad\qquad + \left(G^{\mathrm{T}}(x^k)\right)^+ \lambda^p, \\ 0 = -\nabla_\lambda L(\Delta x^p, \lambda^p) = -C_I(x^k) - G(x^k)\Delta x^p, \end{cases} \tag{22}$$

where p is the number of iterations for QP subproblems. Define $z = (\Delta x, \lambda)^{\mathrm{T}}$ and the KKT operator for the problem which is monotone

$$T(\Delta x^p, \lambda^p) = \begin{bmatrix} \partial_{\Delta x} L(\Delta x^p, \lambda^p) \\ -\left(\nabla_\lambda L(\Delta x^p, \lambda^p)\right)^+ \end{bmatrix}, \tag{23}$$

The iterative process of the primal-dual subgradient method is as follows:

$$z^{p+1} = z^p - \alpha_p T^p, \tag{24}$$

where $T^p \in T(z^p)$ and α_p is the step length.

C. GRADIENT OF OBJECTIVE FUNCTION AND CONSTRAINTS

The given gradient instead of the one calculated by the difference method can make the optimization problem converge to the stationary point more quickly. The gradient of the objective function (18) is derived as

$$P(x) = H_k \Delta x + \nabla F_i(x)|_{i\in I(x)}, \tag{25}$$

where the Hessian matrix H_k can be updated through BFGS method [32]. Without loss of generality, the gradient of the least square error of i-th SMR corresponding to m configurations, ∇F, is deduced in this section.

$$\nabla F_i = 2\left(\frac{\partial r_i}{\partial x^{\mathrm{T}}}\right)^{\mathrm{T}} r_i = 2J_i^{\mathrm{T}}(\theta, x) r_i, \tag{26}$$

where $r_i = [r_{i1}, \ldots, r_{im}]^{\mathrm{T}}$, and $r_{ij} = f(\theta_j, x) - ym_{ij}$. The analytical expression of the Jacobian matrix $J(\theta, x)$ can be readily acquired via the MDH convention. The gradient of the constraints, $G(x)$, is expressed as

$$G(x) = \begin{bmatrix} \nabla F_1^{\mathrm{T}}(x) - \nabla F_i^{\mathrm{T}}(x)|_{i\in I(x)} \\ \vdots \\ \nabla F_i^{\mathrm{T}}(x) - \nabla F_i^{\mathrm{T}}(x)|_{i\in I(x)} \\ \vdots \\ \nabla F_3^{\mathrm{T}}(x) - \nabla F_i^{\mathrm{T}}(x)|_{i\in I(x)} \\ \nabla c_1^{\mathrm{T}}(x) \\ \vdots \\ \nabla c_l^{\mathrm{T}}(x) \\ \vdots \\ \nabla c_3^{\mathrm{T}}(x) \end{bmatrix}, \tag{27}$$

where $i = 1, 2, 3$ is the number of the constraints introduced from the minimax problem into the minimal problem, correspondingly, $l = 1, 2, 3$ generated by physical limitations. The former item can be readily derived by the formula (26), the latter is deduced as below

$$\nabla c_l = 2rt_l \frac{\partial rt_l}{\partial x}, \tag{28}$$

Without loss of generality, only the gradient of the first constraint is considered, and the $\frac{\partial rt_1}{\partial x}$ can be deduced as

$$\frac{\partial rt_1}{\partial x} = \frac{\partial (ta - tb)^{\mathrm{T}}}{\partial x} \frac{(ta - tb)}{\|ta - tb\|}, \tag{29}$$

where $ta = [ta_x, ta_y, ta_z]^{\mathrm{T}}$, and $tb = [tb_x, tb_y, tb_z]^{\mathrm{T}}$ belong to the structural parameters x.

D. CONVEXITY AND CONVERGENCE ANALYSIS

Obviously, the formula (7) is non-convex, since it is the product of a series of matrices containing trigonometric functions. Then, the original objective function (16) is also non-convex, which is the maximum of (7). Through the SQP method, approximately, the original function is replaced by the second-order expansion which can be proved to be convex. According to the Convex Optimization Theory [33], the objective and constraint functions are convex satisfying

$$f(\alpha x + \beta y) \leq \alpha f(x) + \beta f(y), \quad \textit{where } \alpha + \beta = 1,\ \alpha \geq 0,\ \beta \geq 0,$$

Define that

$$Q(\Delta x) = \frac{1}{2} \Delta x^{\mathrm{T}} H_k \Delta x + D_{\Delta x}\phi(x), \tag{30}$$

Then, we have

$$Q(\alpha y + \beta z) - \alpha Q(y) - \beta Q(z) = -\alpha\beta (y - z)^{\mathrm{T}} H_k (y - z) \leq 0, \tag{31}$$

since H_k is a positive definite matrix. So, the objective function in formula (18) is convex. Clearly, the constraints are convex. Then, the conclusion can achieve that the original problem converges to the local minimum. With the step size

$$\alpha_p = \frac{\gamma_p}{\|T^p\|_2}, \gamma_p > 0, \sum_p \gamma_p^2 < \infty,$$

Algorithm 1 Robust Calibration of Kinematic Manipulators

Input: joint angles: θ, nominal parameters: x, measured positions: ym_1, ym_2, ym_3;
Output: optimal parameters: x^*
initialize x^0, H_k
Algorithm initialization:
for j=1:g **do**
$r_i = ym_i - f(\theta, x^0)$
$F_i(x^0) = r_i^{\mathrm{T}} * r_i$
$\nabla F_i(x^0) = 2J^{\mathrm{T}}(\theta, x^0) r_i$
end for
$\phi = max\{F_i\}, I(x^0) = \{i : F_i(x^0) = \phi(x^0)\}$
for j=1:g **do**
$C_I(x^0) \longleftarrow F_i(x^0) - \phi$
$G(x^0) \longleftarrow \nabla F_i(x^0) - \nabla F_i(x^0)|_{i \in I(x^0)}$
end for
for l=1:h **do**
$C_I(x^0) \longleftarrow c_l(x^0) = rt_l^{\mathrm{T}}(x^0) * rt_l(x^0)$
$G(x^0) \longleftarrow \nabla c_l(x^0) = 2Jt^{\mathrm{T}}(x^0) rt_l$
end for
while x not converge **do**
initialize $\Delta x^0 = 0, \lambda^0 = 0$
while Δx not converge **do**
Primal-dual optimal method for QP subproblem:
$$T^p = \begin{bmatrix} H_k \Delta x^p + \nabla F_i(x^k)|_{i \in I} + \left(G^{\mathrm{T}}(x^k)\right)^+ \lambda^p \\ -\left(C_I(x^k) + G(x^k)\Delta x^p\right)^+ \end{bmatrix}$$
$$\alpha_p = \frac{\gamma_p}{\|T^p\|_2}$$
$$z^{p+1} = z^p - \alpha_p T^p$$
end while
States updating:
$x^{k+1} = x^k + \Delta x^k$
$\phi = max\{F_i(x^{k+1})\}$
$I(x^{k+1}) = \{i : F_i(x^{k+1}) = \phi(x^{k+1})\}$
Constraint and gradient matrices updating:
$\nabla F_i(x^{k+1}), C_I(x^{k+1}), G(x^{k+1}) \longleftarrow x^{k+1}$
Hessian matrix updating through BFGS method:
$s^k = \Delta x^k$
$$q_k = \nabla F_i(x^{k+1})|_{i \in I(x^{k+1})} + G^T(x^{k+1})\lambda^{k+1} - [\nabla F_i(x^k)|_{i \in I(x^k)} + G^T(x^k)\lambda^k]$$
$$H_{k+1} = H_k + \frac{q_k q_k^{\mathrm{T}}}{q_k^{\mathrm{T}} s_k} - \frac{H_k s_k s_k^{\mathrm{T}} H_k^{\mathrm{T}}}{s_k^{\mathrm{T}} H_k s_k}$$
end while

the QP subproblem can get convergence [33]:

$$Q(\Delta x^p) \to q^*, \left(C_I(x) + G(x)\Delta x^p\right) \to 0.$$

Hence, with primal-dual optimal method, the osculating quadratic subproblem is able to converge to global minimum for estimating model parameters, and the proposed robust calibration algorithm can converge to the local minimum.

E. INITIAL VALUES OF OPTIMIZATION PROBLEM

The last section has the conclusion that the original problem converges to the local minimum by the SQP method.

TABLE 2. DH parameters of ABB 2600 Robot Manipulator.

♯	a	d	θ	α
1	150	445	0	$-\pi/2$
2	900	0	$-\pi/2$	0
3	150	0	0	$-\pi/2$
4	0	938	0	$\pi/2$
5	0	0	π	$\pi/2$
6	0	200	0	0

Hence, it is crucial to find a suitable initial value for the optimization problem. In plain sight, minimizing the sum of all square errors is a suitable choice, and the optimization problem can be expressed as

$$\begin{aligned} &\underset{x}{minimize}: \ F_1(x) + F_2(x) + F_3(x), \\ &subject\ to: \ c(x) \le 0 \end{aligned} \tag{32}$$

where the optimal solution x^* can be readily gained using Gauss-Newton Method and be set as initial values of the minimax problem.

F. ALGORITHM DESIGN AND ANALYSIS

Algorithm Robust Calibration gives the pseudo code of the proposed robust calibration method. The section III-E gives an appropriate initial value x^0 for the iterative optimization problem. Then, approximately, the original function (7) is replaced by the second-order expansion through the SQP method, and the corresponding constraint matrix C_I and gradient matrices $\nabla F, G$ can be calculated by substituting the initial value x^0. During the iterative process, the second-order expansion, namely the QP subproblem, is continuously recalculated and updated as the structural parameter x changes. In each iteration process of x, the QP subproblem is solved by the primal-dual optimal method.

IV. EXPERIMENTAL VERIFICATION

Note that ABB IRB 2600 is commonly used in industrial applications [34], [35], and its structural parameters expressed in the form of a MDH model can be readily compensated back to the controller through the file *absacc.cfg*. Besides, the ABB IRB 2600 with six independent joints can reach any position in the working space at any orientation. In this section, the proposed method will be experimentally validated on the IRB 2600 manipulator whose nominal structural parameters are shown in TABLE 2, and the positions of the end point are measured by the laser tracker (FARO Vantage) with the accuracy of $10\mu m + 2.5\mu m/m$ as shown in Fig. 1.

A. ACQUISITION OF THE POSITION DATA

To show the efficacy of the proposed algorithm and guarantee the manipulator accuracy in the global workspace, a total of 100 configurations are arbitrarily selected for the calibration. Initially, transformation from measurement coordinate system to base, and the coordinates *ta*, *tb* and *tc* are calculated

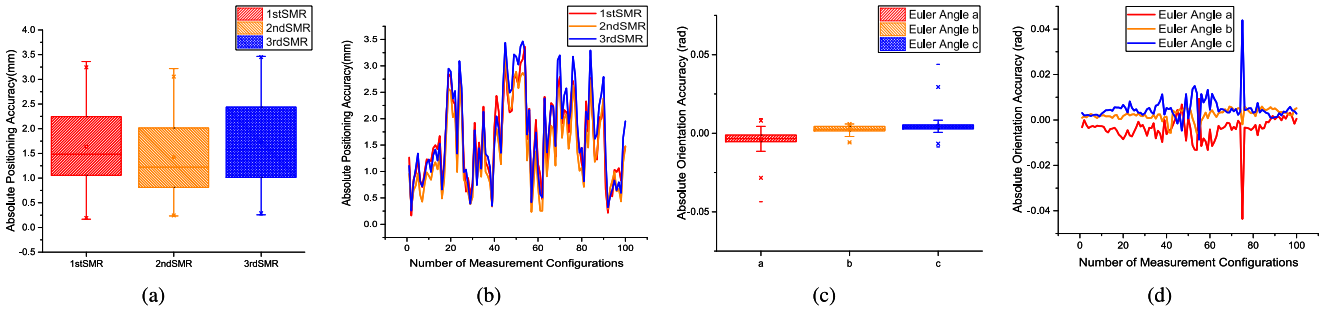

FIGURE 2. Experimental results of absolute positioning (*AP*) accuracy and absolute orientation (*AO*) accuracy with nominal structural parameters. (a) Box chart of the *AP* accuracy corresponding to three SMRs. (b) 2D map of the *AP* accuracy. (c) Box chart of the *AO* accuracy. (d) 2D map of the *AO* accuracy.

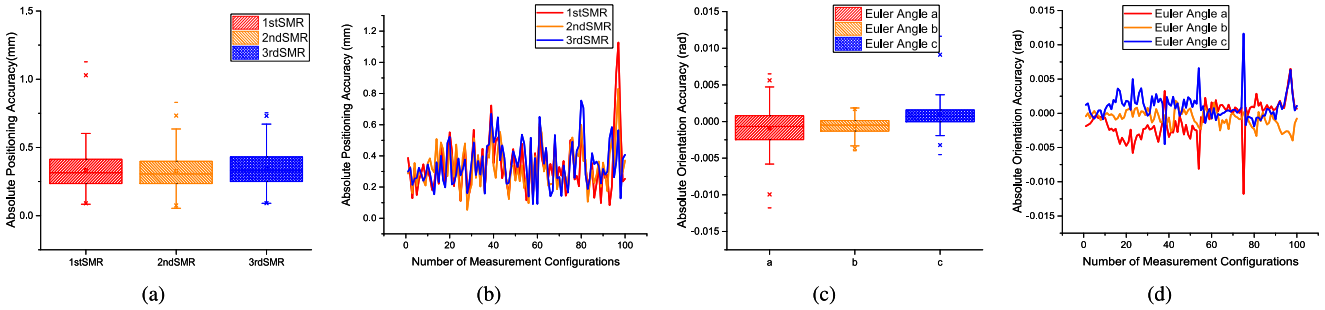

FIGURE 3. Experimental results of *AP* accuracy and *AO* accuracy with both structural parameters and coordinate systems attained by the minimax search algorithm. (a) Box chart of the *AP* accuracy corresponding to three SMRs. (b) 2D map of the *AP* accuracy. (c) Box chart of the *AO* accuracy. (d) 2D map of the *AO* accuracy.

as the initial value, and the method can be found in [36]. Then, the manipulator automatically moves to the selected configuration one after another, and pauses 10 seconds between two configurations. In the meantime, the approximate positions of SMRs can be calculated with the initial transformations and joint angles, and the laser tracker can quickly search for the target SMR with the position information. When the manipulator reaches the command configuration, a startup message is sent to the laser tracker for measurement. Once the position data is attained, a message is returned back to the manipulator for the next move. Finally, the positions of three SMRs responding to 100 configurations can be attained within 30 minutes, and the corresponding joint angles can be read through the controller of the manipulator.

B. CALIBRATION WITH MINIMAX SEARCH ALGORITHM

With all the data attained, the minimax algorithm can search for the optimal structural parameters x. Fig. 2 show the initial absolute positioning and orientation accuracy before calibration, while Fig. 3 show the final after calibration, respectively. It can be seen from the experimental results that the minimax search algorithm dramatically improves the positioning and orientation accuracy of the manipulator by 67.34% and 73.14%, respectively. Analysis of the orientation accuracy in Fig. 2(d) and 3(d) can be found that the orientation error of the 75th point is particularly large. According to the characteristics of the orientation accuracy given in Sec. II-C, it is likely that the Euler angle is near the singular value in this configuration, resulting in a large orientation error. Using the newly defined orientation accuracy indicator in formula (5), the comparison of modified orientation accuracy before and after calibration is represented in Fig. 4, improved by 32.76%. However, the root mean square error (RMSE) is more able to reflect the degree of dispersion of the deviation between actual arrival pose and command pose, and the RMSE of orientation before and after calibration is 0.005015 *rad* and 0.002176 *rad*, respectively.

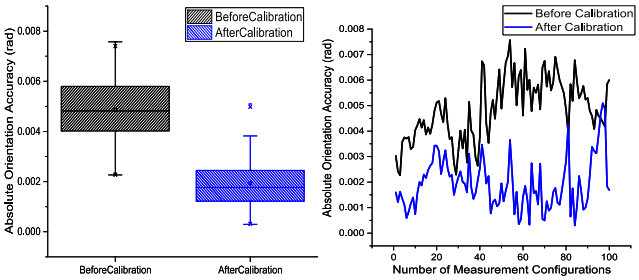

FIGURE 4. Comparison of modified orientation accuracy before and after calibration. (a) Box chart of accuracy comparison. (b) 2D map of accuracy comparison.

C. COMPARISONS WITH EXISTING METHODS

The experimental results calculated under different conditions are shown in the Fig. 5, and corresponding data is in the Tab. 3, where condition 0 indicates the situation

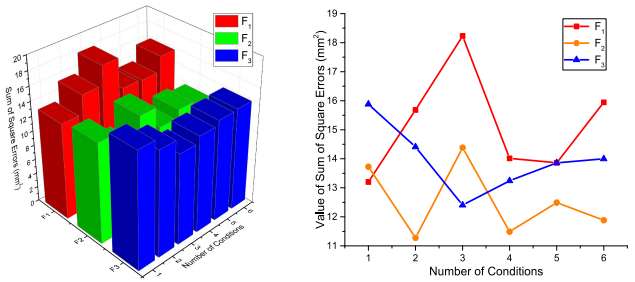

(a) (b)

FIGURE 5. Sum of square errors of three SMRs under different conditions: Condition 1, minimize the value of F_1; Condition 2, minimize F_2; Condition 3, minimize F_3; Condition 4, minimize $\{F_1 + F_2 + F_3\}$; Condition 5, minimize $max\{F_i\}$; Condition 6, minimize pose errors.

TABLE 3. Sum of square errors corresponding to different methods.

Conditions	0	1	2	3	4	5	6
F_1/mm^2	325.90	13.20	15.68	18.23	14.02	13.86	15.94
F_1/mm^2	261.23	14.72	11.27	14.38	11.49	12.49	11.88
F_3/mm^2	373.88	15.88	14.41	12.40	13.24	13.86	14.00
RMSE(ϕ)/mm	1.934	0.399	0.396	0.427	0.374	0.372	0.399
Methods	Original	[18], [19]	[18], [19]	[18], [19]		This paper	[28]

before calibration. From these results it is clear that the maximal root mean square error of three SMRs, $RMSE(\phi)$, is minimal with the proposed method. Contrary to the results of calibration with only one SMR, namely condition 1 to 3, it can be concluded that single-SMR calibration can reduce the RMSE of SMRs not involved in the calibration to a certain extent, but the effect is not as good as the proposed method. Condition 6 is the scheme that directly minimizes the square sum of the positioning and orientation errors, and its maximal root mean square error of three SMRs is still larger than the proposed method.

In order to further verify the improvement of absolute positioning and orientation accuracy with various methods, box charts of the absolute accuracy under different condition are shown in the Fig. 6. Compared to the single-SMR calibration, the absolute positioning and orientation accuracy are developed by 23.48% and 22.30%, respectively, with the proposed method. Compared with the method directly calculating and minimizing positioning and orientation errors, namely pose errors, although the orientation accuracy of the proposed method is slightly inferior to the method of directly minimizing the pose, the positioning accuracy is still significantly improved by 14.36%.

D. VERIFICATION ON OTHER MANIPULATORS

In order to verify the versatility of the proposed algorithm, the algorithm was tested on two other manipulators, and the experimental results compared with previous works are shown in the TABLE 4. From the table, it can be concluded that the proposed method has the best positioning accuracy compared with the previous works. As for the orientation accuracy, the method in this paper is better than single-SMR

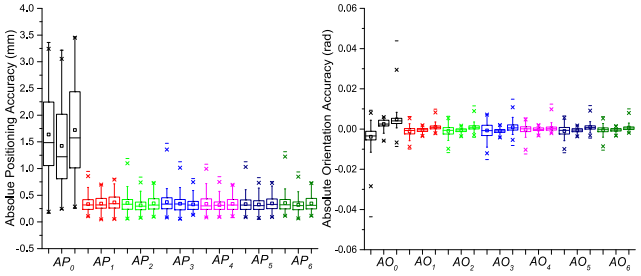

(a) (b)

FIGURE 6. Box chart of the absolute accuracy corresponding to different conditions. (a) The absolute positioning accuracy to different conditions, abbreviated to AP_i, (b) the absolute orientation accuracy to different conditions, abbreviated to AO_i. The subscript $i = 0, \ldots, 6$ indicates the number of conditions. Three bars of the box chart corresponding to each condition represent the positioning accuracy of three SMRs for AP_i, and the orientation accuracy of Euler angle for AO_i, respectively.

TABLE 4. Experimental results corresponding to different methods.

		Methods	Original	This paper	[18], [19]	[28]
SR10	Positioning	RSME(ϕ)/mm	16.07	0.206	0.207	0.207
	accuracy	Max/mm	18.35	0.554	0.600	0.600
	Orientation	RSME(ϕ)/rad	0.048	0.0018	0.0018	0.0018
	accuracy	Max/rad	0.292	0.0048	0.0053	0.0044
IRB2600	Positioning	RSME(ϕ)/mm	1.901	0.3323	0.3471	0.3431
	accuracy	Max/mm	3.404	0.9612	1.1298	0.9894
	Orientation	RSME(ϕ)/rad	0.0048	0.0026	0.0027	0.0025
	accuracy	Max/rad	0.0250	0.0117	0.0121	0.0101

method proposed in [18], [19], and slightly inferior to the method proposed in [28].

V. CONCLUSIONS

In this paper, an autonomous kinematic calibration method with pose information considered is proposed, which consists of four parts: pose measurement, modeling, identification and compensation. The novel feature is that, in the identification procedures, by optimizing the worst case of the three points mounted on the end-effector, both absolute positioning and orientation accuracy of manipulators can be improved, and in the meantime, the robustness of the calibration process is increased. Besides, the method is based on a simple set of sensing data, which reduces the manual operation in data collection. Compared with vision based measurement method, this method reduces error propagation due to orientation calculation and coordinate transformation. Before ending this paper, it worth mentioning that the proposed algorithm is able to successfully address robust calibration problem of manipulators and the experimental results based on IRB 2600 robot show that both positioning and orientation accuracy are improved by 67.34% and 73.14%, respectively. Moreover, the proposed method has the best positioning accuracy compared with the previous works [18], [19], [28].

REFERENCES

[1] H. Do, C. Park, and J. H. Kyung, "Dual arm robot for packaging and assembling of IT products," in *Proc. IEEE Int. Conf. Autom. Sci. Eng.*, Aug. 2012, pp. 1067–1070.

[2] H. Chen, J. Wang, G. Zhang, T. Fuhlbrigge, and S. Kock, "High-precision assembly automation based on robot compliance," *Int. J. Adv. Manuf. Technol.*, vol. 45, nos. 9–10, pp. 999–1006, May 2009.
[3] Y. Li and B. Hannaford, "Gaussian process regression for sensorless grip force estimation of cable-driven elongated surgical instruments," *IEEE Robot. Autom. Lett.*, vol. 2, no. 3, pp. 1312–1319, Jul. 2017.
[4] Z. Pan, H. Zhang, Z. Zhu, and J. Wang, "Chatter analysis of robotic machining process," *J. Mater. Process. Technol.*, vol. 173, no. 3, pp. 301–309, Apr. 2006.
[5] C. Chen, P. Chen, and C. Hsu, "Three-dimensional object recognition and registration for robotic grasping systems using a modified viewpoint feature histogram," *Sensors*, vol. 16, no. 11, p. 1969, Nov. 2016.
[6] M. Suzuki, K. Noda, Y. Suga, T. Ogata, and S. Sugano, "Dynamic perception after visually guided grasping by a human-like autonomous robot," *Adv. Robot.*, vol. 20, no. 2, pp. 233–254, Jan. 2006.
[7] A. Joubair and I. A. Bonev, "Kinematic calibration of a six-axis serial robot using distance and sphere constraints," *Int. J. Adv. Manuf. Technol.*, vol. 77, nos. 1–4, pp. 515–523, Mar. 2015.
[8] R. Wang, G. Yang, H. Zhao, and J. Luo, "Robot kinematic calibration with plane constraints based on POE formula," in *Proc. IEEE Int. Conf. Inf. Autom.*, Feb. 2017, pp. 1887–1892.
[9] S. He, L. Ma, C. Yan, C. Lee, and P. Hu, "Multiple location constraints based industrial robot kinematic parameter calibration and accuracy assessment," *Int. J. Adv. Manuf. Technol.*, vol. 102, no. 5, pp. 1037–1050, Jun. 2018.
[10] L. Ma, P. Bazzoli, P. Sammons, R. Landers, and D. Bristow, "Modeling and compensation of joint-dependent kinematic errors in robotic manipulators," in *Proc. Int. Symp. Flexible Autom.*, Aug. 2016, pp. 458–464.
[11] J. Miseikis, K. Glette, O. Elle, and J. Torresen, "Automatic calibration of a robot manipulator and multi 3D camera system ," in *Proc. IEEE/SICE Int. Symp. Syst. Integr.*, Dec. 2017, pp. 735–741.
[12] W. Chen, J. Du, W. Xiong, Y. Wang, S. Chia, B. Liu, and Y. Gu, "A noise-tolerant algorithm for robot-sensor calibration using a planar disk of arbitrary 3-D orientation," *IEEE Trans. Autom. Sci. Eng.*, vol. 15, no. 1, pp. 251–263, Jan. 2018.
[13] Y. Ren, S. Yin, and J. Zhu, "Calibration technology in application of robot-laser scanning system," *Opt. Eng.*, vol. 51, no. 11, p. 4204, Nov. 2012.
[14] J. Li, M. Chen, X. Jin, Y. Chen, Z. Dai, Z. Ou, and Q. Tang, "Calibration of a multiple axes 3-D laser scanning system consisting of robot, portable laser scanner and turntable," *Optik*, vol. 122, no. 4, pp. 324–329, Feb. 2011.
[15] X. Yang, L. Wu, J. Li, and K. Chen, "A minimal kinematic model for serial robot calibration using POE formula," *Robot. Comput.-Integr. Manuf.*, vol. 30, no. 3, pp. 326–334, Jun. 2014.
[16] Y. Meng and H. Zhuang, "Autonomous robot calibration using vision technology," *Robot. Comput.-Integr. Manuf.*, vol. 23, no. 4, pp. 436–446, Aug. 2007.
[17] J. M. S. T. Motta, G. Carvalho, and R. S. Mcmaster, "Robot calibration using a 3D vision-based measurement system with a single camera," *Robot. Comput.-Integr. Manuf.*, vol. 17, no. 6, pp. 487–497, Dec. 2001.
[18] S. H. Ye, Y. Wang, Y. J. Ren, and D. K. Li, "Robot calibration using iteration and differential kinematics," *J. Phys. Conf. Ser.*, vol. 48, no. 1, pp. 1–6, 2006.
[19] X. Yang, D. Liu, Y. Bai, M. Cong, and Z. Liao, "Kinematics calibration research based on the positioning error of the 6-DOF industrial robot," in *Proc. IEEE Int. Conf. Cyber Technol. Autom.*, Jun. 2015, pp. 913–917.
[20] G. Chen, H. Wang, and Z. Lin, "Determination of the identifiable parameters in robot calibration based on the POE formula," *IEEE Trans. Robot.*, vol. 30, no. 5, pp. 1066–1077, Oct. 2014.
[21] L. Wu, X. Yang, K. Chen, and H. Ren, "A minimal poe-based model for robotic kinematic calibration with only position measurements," *IEEE Trans. Autom. Sci. Eng.*, vol. 12, no. 2, pp. 758–763, Apr. 2015.
[22] X. Zhang, Y. Song, Y. Yang, and H. Pan, "Stereo vision based autonomous robot calibration," *Robot. Auto. Syst.*, vol. 93, pp. 43–51, Jul. 2017.
[23] S. Li, H. Wang, and M. U. Rafique, "A novel recurrent neural network for manipulator control with improved noise tolerance," *IEEE Trans. Neural Netw. Learn. Syst.*, vol. 29, no. 5, pp. 1908–1918, May 2017.
[24] S. Li, M. Zhou, and X. Luo, "Modified primal-dual neural networks for motion control of redundant manipulators with dynamic rejection of harmonic noises," *IEEE Trans. Neural Netw. Learn. Syst.*, vol. 29, no. 10, pp. 4791–4801, Oct. 2018.
[25] Y. Li, S. Li, and B. Hannaford, "A model-based recurrent neural network with randomness for efficient control with applications," *IEEE Trans. Ind. Inform.*, vol. 15, no. 4, pp. 2054–2063, Apr. 2018.
[26] L. Jin, S. Li, X. Luo, Y. Li, and B. Qin, "Neural dynamics for cooperative control of redundant robot manipulators," *IEEE Trans. Ind. Inform.*, vol. 14, no. 9, pp. 3812–3821, Sep. 2018.
[27] Y. Li, S. Li, and B. Hannaford, "A novel recurrent neural network for improving redundant manipulator motion planning completeness," in *Proc. IEEE Int. Conf. Robot. Autom.*, May 2018, pp. 2956–2961.
[28] X. Wang, D. Li, and M. Wang, "Complete calibration of industrial robot with limited parameters and neural network," in *Proc. IEEE Int. Symp. Robot. Intell. Sensors*, Dec. 2016, pp. 103–108.
[29] K. Madsen and H. Schjaer-Jacobsen, "Algorithms for worst-case tolerance optimization," *IEEE Trans. Circuits Syst.*, vol. 26, no. 9, pp. 775–783, Sep. 1979.
[30] J. Bonnans, J. Gilbert, C. Lemarechal, and C. Sagastizabal, "Numerical optimization–theoretical and practical aspects," *IEEE Trans. Autom. Control*, vol. 51, no. 3, p. 541, Aug. 2003.
[31] Y. Zhang and J. Wang, "A dual neural network for convex quadratic programming subject to linear equality and inequality constraints," *Phys. Lett. A*, vol. 298, no. 4, pp. 271–278, 2002.
[32] R. Cottle and M. Thapa, *Linear and Nonlinear Optimization*. New York, NY, USA: Springer,2017.
[33] S. Boyd and L. Vandenberghe, *Convex Optimization*. London, U.K.: Cambridge Univ. Press, 2004.
[34] N. Doan, W. Lin, and P. Tao, "Optimal redundancy resolution for robotic arc welding using modified particle swarm optimization," in *Proc. IEEE Int. Conf. Adv. Intell. Mechatron.*, Jul. 2016, pp. 554–559.
[35] H. Fang, S. Ong, and A. Nee, "Robot path planning optimization for welding complex joints," *Int. J. Adv. Manuf. Technol.*, vol. 90, no. 9, pp. 3829–3239, Jun. 2016.
[36] F. Dornaika and R. Horaud, "Simultaneous robot-world and hand-eye calibration," *IEEE Trans. Robot. Automat.*, vol. 14, no. 4, pp. 617–622, Aug. 1998.

CHENTAO MAO received the B.E. degree in mechatronic engineering from the University of Electronic Science and Technology of China, Chengdu, China, in 2015. He is currently pursuing the Ph.D. degree in mechanical electronics with the Department of Mechanical Engineering, Zhejiang University, Hangzhou, China. His current research interests include kinematic calibration, optimization theory, and control.

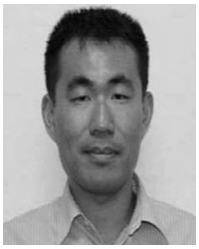

SHUAI LI (M'14–SM'17) received the B.E. degree in precision mechanical engineering from the Hefei University of Technology, Hefei, China, the M.E. degree in automatic control engineering from the University of Science and Technology of China, Hefei, and the Ph.D. degree in electrical and computer engineering from the Stevens Institute of Technology, Hoboken, NJ, USA. He is currently an Associate Professor in robotics and autonomous systems with the College of Engineering, Swansea University, U.K. His current research interests include robot arm manipulation and calibration, impedance/admittance control, human–robot interaction, and dynamic neural networks. He served as the General Co-Chair of the 2018 International Conference on Advanced Robotics and Intelligence Control, and currently serves as the Editor-in-Chief of the *International Journal of Robotics and Control*.

ZHANGWEI CHEN received the B.S. degree in scientific instruments and the Ph.D. degree in mechanical engineering from Zhejiang University, Hangzhou, China, in 1986 and 1995, respectively.

He is currently a Professor with the Faculty of Mechanical Engineering and Automation, Zhejiang University. His research interests include vibration and control, signal sensing and analysis, and robot properties' measurement and calibration.

HONGFEI ZU was born in Linyi, Shandong, China, in 1985. He received the B.S. degree in micro-electronics and the M.S. degree in electronics science and technology from Xian Jiaotong University, Xian, China, in 2009 and 2012, respectively, and the Ph.D. degree in mechanical engineering and materials science from the University of Pittsburgh, Pittsburgh, PA, USA, in 2017.

He was an Assistant Professor with the Sichuan University-Pittsburgh Institute (SCUPI), from 2017 to 2018. He is currently an Associate Professor with the Faculty of Mechanical Engineering and Automation, Zhejiang Sci-Tech University. His research interests include piezoelectric sensors, especially high-temperature sensor and surface acoustic wave (SAW) and bulk acoustic wave (BAW) sensor applications, and robot properties' measurement and calibration.

ZHIRONG WANG received the B.E. degree in computer science from Changzhou University, Changzhou, China, in 2013, and the master's degree in computer application technology from the Nanjing University of Science and Technology, Nanjing, China, in 2016. He is currently pursuing the Ph.D. degree with the College of Mechanical Engineering, Zhejiang University.

His current research interests include robot kinematics, dynamics, and control.

YUXIANG WANG received the B.E. degree in mechanical engineering from Zhengzhou University, Zhengzhou, China, in 2014. He is currently pursuing the Ph.D. degree in mechanical electronics with the Department of Mechanical Engineering, Zhejiang University, Hangzhou, China.

His current research interests include robot calibration, dynamics, and neural networks.